03,13

Ab initio Calculations of Phonon Spectra and Thermal Conductivity in RhSi, RhSn and Solid Solutions Based on them

© M.R. Sharnas[1,2], D.A. Pshenay-Severin[1,¶], A.T. Burkov[1]

[1] Ioffe Institute,
St. Petersburg, Russia
[2] Peter the Great Saint-Petersburg Polytechnic University,
St. Petersburg, Russia

¶ E-mail: d.pshenay@mail.ru

Received March 13, 2024
Revised April 25, 2024
Accepted April 27, 2024

Cobalt monosilicide and its solid solutions are promising thermoelectrics, as they have a high thermoelectric power factor and mechanical strength. To increase the thermoelectric efficiency of these materials, it is necessary to reduce their lattice thermal conductivity. This work examines the possibility of such reduction using the solid solution approach. Using ab initio calculations, phonon spectra, total and projected densities of phonon states of isostructural to CoSi compounds RhSi and RhSn were obtained. All these compounds have B20 structure of FeSi type. Calculations of the temperature dependence of the thermal conductivity of these crystals, as well as CoSi-RhSi and RhSi-RhSn solid solutions, were carried out. Calculations showed that the lattice thermal conductivity at room temperature in RhSi was 4.9 W/(m · K), and in RhSn — 3.6 W/(m · K), which is significantly lower than in pure CoSi (about 10.4 W/(m · K)). Due to additional alloy scattering in CoSi-RhSi solid solutions, thermal conductivity can be reduced by more than 3 times compared to pure CoSi, and in RhSi-RhSn solid solutions by more than 3 times compared to a pure RhSi crystal.

Keywords: lattice thermal conductivity, thermoelectrics, ab initio lattice dynamics.

DOI: 10.61011/PSS.2024.05.58495.54

1. Introduction

For wider range of applications of thermoelectric generators, it is necessary to search for materials with high efficiency of energy conversion. Cobalt monosilicide (CoSi) is one of the promising materials for medium-temperature thermoelectric generators. CoSi crystallizes in B20 noncentrosymmetric structure (space group $P2_13$) [1,2]. It has thermopower that is high for a semimetal (about $-80\,\mu$V/K) and a high thermoelectric power factor of 5.5 mW/(m · K) that exceeds that of a well known thermoelectric material — bismuth telluride [1,2]. CoSi contains low-cost and nontoxic components and is stable at high temperatures. However, despite the high power factor, the lattice thermal conductivity in a pure crystal is too high: $\kappa = 10.4-12.3$ W/(m · K) at room temperature [1,3]. Thermal conductivity can be reduced using the solid solutions method. For example, in works [1,4,5], non-isovalent substitution of Co by Fe or Ni atoms was studied. Addition of 5 at.% Fe (4 at.% Ni) allowed thermal conductivity to be reduced from 10.4 to 7.9(9.2) W/(m · K), i. e. by 24% (12%) [1]. Transport properties of isostructural CoGe and its solid solutions with Co substituted by Fe(Ni) were studied in [6,7]. This material also has thermopower that is high for a semimetal and is equal to about $-80\,\mu$V/K, but much lower lattice thermal conductivity — about 5.3 W/(m · K) [7], that is associated with a higher weight of germanium atoms compared with silicon atoms. In addition to non-isovalent solid solutions, alloys with isovalent substitution of Co by Ge in CoSi were examined [8–10]. Due to significant difference in atomic masses of substituted atoms, thermal conductivity decreased to 7.3 W/(m · K), i. e. by approx 30%, even at 3 at.% of Ge. *Ab initio* calculations of lattice thermal conductivity in CoSi-CoGe solid solutions performed in [10] agree well with the available experimental data and suggest that lattice thermal conductivity in these solid solutions can be approximately twice as low as in CoSi when Ge concentration is only 10−15%.

Therefore, it is also interesting to study lattice transport properties of other materials that are isostructural to CoSi. Using the band structure and material stability data [2,11], rhodium silicide and stannide were chosen for the study. Their phonon spectra, lattice thermal conductivities and also thermal conductivities of CoSi-RhSi and RhSi-RhSn solid solutions were investigated. Due to considerable difference in atomic masses of Rh and Co atoms (approximately by a factor of 2) and of Si and Sn, high reduction of lattice thermal conductivity may be expected, in particular, in solid solutions, due to additional phonon scattering on point defects.

2. Methods for calculating phonon spectra and lattice thermal conductivity

Lattice properties of pure RhSn and RhSi crystals were calculated using the density functional theory implemented

in QuantumESPRESSO (QE) [12,13] and VASP packages [14,15]. The calculations used local approximation for density functional with gradient corrections (GGA) in PBE [16] and PBEsol [17] versions. Calculations in QuantumESPRESSO (VASP) were performed using a cutoff energy of 80Ry (400 eV). For integration over the Brillouin zone, a $6 \times 6 \times 6$ grid in k-space and Gaussian smoothing with a peak FWHM of 0.026 eV were used. The threshold for leaving self-consistency cycle corresponded to a change in total energy by a value lower than 10^{-9} eV per atom, interatomic force relaxation threshold was equal to 10^{-4} eV/Å. Parameters of calculation ensure convergence of total energy better than 1 meV per atom and of interatomic forces better than 1 meV/Å. B20 cubic structure (FeSi type), in which the given materials crystallize, has the following parameters: lattice constant a_0 and atom positions inside the lattice cell. Rh and Si atoms in RhSi (Rh and Sn atoms in RhSn) are in 4a-positions with (x, x, x), $(-x + 1/2, -x, x + 1/2)$, $(-x, x + 1/2, -x + 1/2)$, $(x + 1/2, -x + 1/2, -x)$ coordinates, where $x = x_{\mathrm{Rh(Si,Sn)}}$. Lattice parameters calculated after relaxation are listed in the table in comparison with the experimental data.

The table shows that the calculations made in different packages for the same functionals are very close. Lattice constants calculated in PBE approximation exceed the experimental data by about 1 percent and, when using PBEsol functional, the deviation from the experiment is equal to fractions of a percent. Thus, PBEsol appears to be more preferable for these materials and the main results were obtained in this approximation.

To calculate lattice properties of pure RhSn and RhSi crystals, it is necessary to determine the 2-nd and 3-rd order force constants occurring in the expansion of the total energy in series with respect to small atomic displacements from equilibrium. Force constants connect the interatomic forces, that appear due to atomic displacements from equilibrium lattice positions, with the displacement components. The method of finite displacements in supercell offers one of the ways to calculate them. This method creates a supercell from several unit cells with a sufficient size such that the interatomic interactions decrease to negligibly low values at the supercell size. Then, it is necessary to set displacements from the equilibrium for one atom or a pair of atoms and determine the resulting interatomic forces using *ab initio* calculations. By completing this procedure for a set of atomic configurations, we obtain a system of equations connecting forces and displacements from which the 2-nd and 3-rd order force constants may be found. This method is implemented in PhonoPy and Phono3Py software [20,21].

To calculate the 2-nd and 3-rd order force constants, $3 \times 3 \times 3$ and $2 \times 2 \times 2$ supercells were used, respectively.

Thermal conductivity of RhSi and RhSn was calculated using three-phonon scattering processes in relaxation time approximation. Calculations were performed on the $19 \times 19 \times 19$ grid in k-space to ensure convergence with respect to thermal conductivity better than 0.1 W/(m · K).

Lattice thermal conductivity in solid solutions was calculated using *ab initio* approach that combined the virtual crystal and lattice dynamics methods (virtual crystal *ab initio* lattice dynamics, VC-ALD) [22–25]. This method is based on using lattice constants, force constants and atomic masses for pure substances constituting the solid solution followed by linear interpolation to determine the required parameters for the given composition. In addition, alloy scattering in solid solutions is considered due to phonon scattering associated with the difference in masses of the substituted elements. The method was successfully used to calculate thermal conductivity of solid solutions in a set of thermoelectric materials [22–25].

It was shown in [24] that this method provides good results if there is no abnormally high contribution of high-frequency phonons to thermal conductivity because, when such contribution is present, thermal conductivity is highly underestimated due to reduction of the relaxation time for high-frequency phonon scattering on point defects. As shown below, contribution of high-frequency phonons in RhSn and RhSi to thermal conductivity is low. This suggests that this method will give adequate estimates of thermal conductivity in considered solid solutions of CoSi-RhSi and RhSi-RhSn. For isostructural CoSi-CoGe solid solutions, this method was used in [10] and showed good agreement with the available experimental data for lattice thermal conductivity. Lattice constants and force constants for CoSi that are required to calculate thermal conductivity of CoSi-RhSi solid solutions were taken from [10].

Comparison of the experimental and calculated lattice parameters of RhSi and RhSn (see explanations in the text) obtained in QuantumESPRESSO (QE) and VASP using PBE and PBEsol approximations for density functional

Crystal	a_0, Å (error, %)	x_{Rh}	$x_{\mathrm{Si(Sn)}}$
RhSi, exp. [18]	4.675	0.144	0.840
RhSi, PBE, QE	4.719 (0.95%)	0.152	0.842
RhSi, PBE, VASP	4.719 (0.95%)	0.152	0.842
RhSi, PBEsol, QE	4.676 (0.01%)	0.153	0.842
RhSi, PBEsol, VASP	4.674 (−0.03%)	0.153	0.842
RhSn, exp. [19]	5.122	–	–
RhSn, PBE, QE	5.197 (1.47%)	0.143	0.840
RhSn, PBE, VASP	5.203 (1.58%)	0.143	0.840
RhSn, PBEsol, QE	5.128 (0.11%)	0.145	0.840
RhSn, PBEsol, VASP	5.137 (0.29%)	0.145	0.840

3. Calculation results

Phonon spectra and partial density of phonon states for RhSi and RhSn are shown in Figures 1 and 2. Since the mass of Rh is more than 3.5 times higher than the mass of Si, contribution to low-frequency vibrations in RhSi is

primarily connected with Rh atoms, while contribution to high-frequency oscillations is connected with Si atoms. The phonon spectrum of RhSn shown in Figure 2 demonstrates maximum lattice vibration frequencies that are approximately twice as low as that of RhSi due to the higher atomic mass of Sn compared with Si. Contributions into the phonon density of states from Rh and Sn atoms are almost the same at all spectral frequencies owing to small difference in their masses.

Thermal conductivity calculations of pure materials took into account three-phonon scattering processes in relaxation time approximation and were performed for both density functionals (PBE and PBEsol). When using the density functional in PBEsol approximation, the calculated lattice thermal conductivity for RhSi was equal to 4.9 W/(m · K) and for RhSn it was equal to 3.6 W/(m · K) at room temperature. For comparison, lattice thermal conductivity was also calculated in PBE approximation resulting in 3.6 W/(m · K) for RhSi and 2.5 W/(m · K) for RhSn. Lower thermal conductivities calculated in PBE-approximation correlate with higher lattice constants (see the table). Both variants of calculations give much lower thermal conductivities compared with that of CoSi. However, better agreement between the lattice constants and experimental data in PBEsol-approximation suggests that the thermal conductivities calculated in this approximation will be closer to the experimental data. Temperature dependences of thermal conductivity for this case are shown in Figure 3 (solid lines).

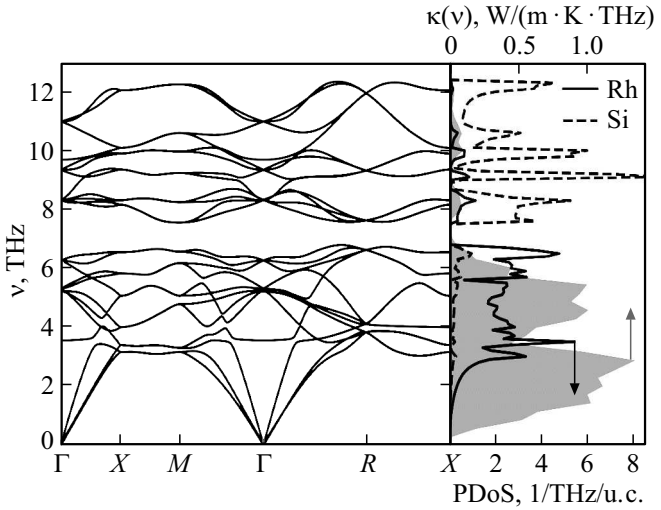

Figure 1. Phonon spectrum of RhSi (on the left), contribution into phonon density of states from Rh and Si vibrations (PDoS, lines on the right) and partial contribution of phonons with various frequency to thermal conductivity ($\kappa(\upsilon)$, filled area on the right).

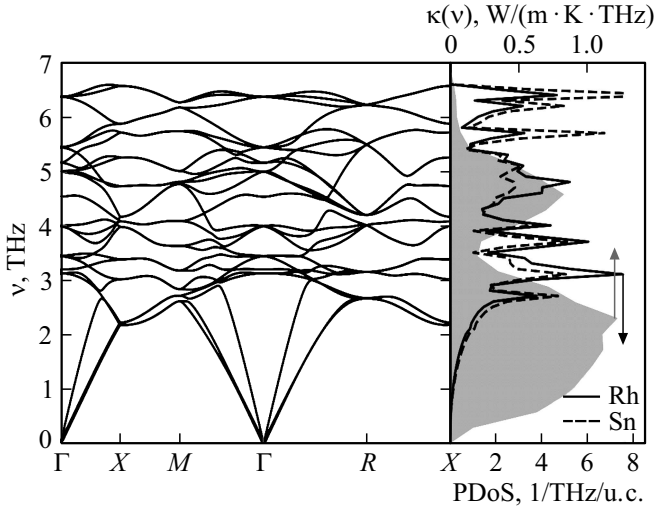

Figure 2. Phonon spectrum of RhSn (on the left), contribution into phonon density of states from Rh and Sn vibrations (PDoS, lines on the right) and partial contribution of phonons with various frequency to thermal conductivity ($\kappa(\upsilon)$, filled area on the right).

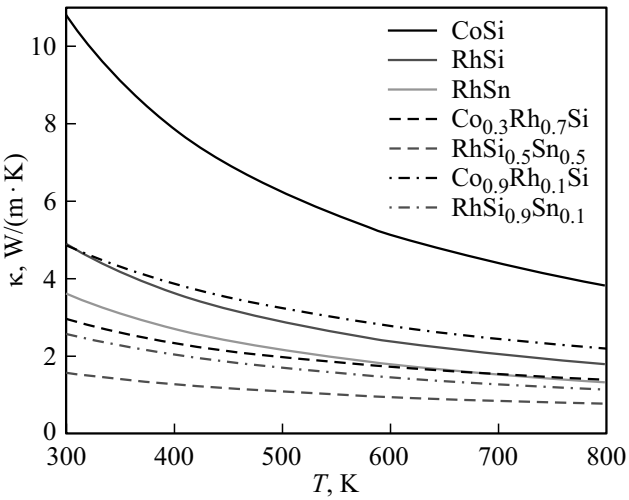

Figure 3. Temperature dependences of lattice thermal conductivity of CoSi [10], RhSi and RhSn and of some $Rh_xCo_{1-x}Si$ and $RhSn_xSi_{1-x}$ solid solutions.

Figures 1 and 2 show the contribution of phonons with different frequencies $\kappa(\upsilon)$ to thermal conductivity of RhSn and RhSi, filled areas on the right, where $\kappa(\upsilon) = \sum_{kj} \kappa_{kj} \delta(\upsilon - \upsilon_{kj})$, where κ_{kj} — is the contribution to thermal conductivity from phonons with wave vector $\boldsymbol{k}$ and mode number j, and $\delta(\upsilon - \upsilon_{kj})$ is the Dirac delta function. The calculated dependences indicate that the main contribution to thermal conductivity in RhSn comes from acoustic phonons corresponding to Rh and Sn atom vibrations with frequencies lower than 3 THz and by phonons within a medium-frequency range from 3 to 6 THz. The main contribution to thermal conductivity of RhSi is also provided by acoustic and medium-frequency optical phonons, but they are primarily associated with Rh vibrations. Whilst optical vibrations with a frequency higher than 7.5 THz associated mainly with Si vibrations make a minor contribution to thermal conductivity.

To identify the effect of phonon spectrum and scattering on the lattice thermal conductivity of pure rhodium silicide and stannide crystals, dependences of speed of sound

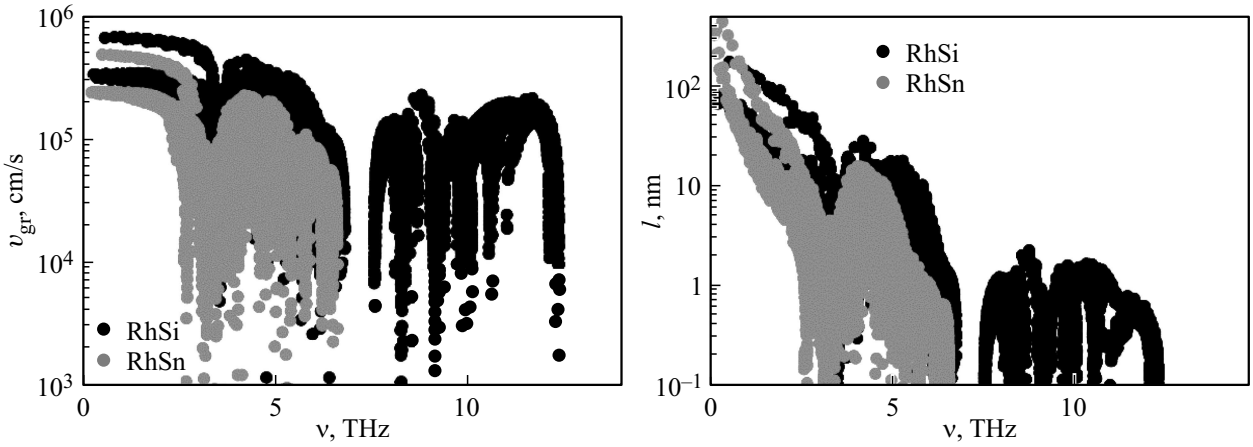

Figure 4. Dependences of group velocity v_{gr} (on the left) and mean free path (on the right) of phonons on frequency in RhSi and RhSn.

and mean free path were plotted at different frequencies (Figure 4), because the lattice thermal conductivity is directly proportional to these two values. It can be seen that the group velocity of phonons in RhSi is higher than that in RhSn at all vibration frequencies and the mean free path in RhSi is also higher than that in RhSn, except at low frequencies. Spectrum in RhSn is limited by frequencies lower than 7 THz. Contribution of phonons with frequencies higher than 7.5 THz in RhSi is small (Figure 1, on the right), that is mainly associated with low mean free path of phonons in this frequency region (Figure 4, on the right).

When using nanostructuring, polycrystalline samples with small grain size are used for thermal conductivity reduction in order to limit the mean free path of phonons due to boundary scattering (see, for example, [26]). To estimate thermal conductivity reduction in such structures, one often use cumulative thermal conductivity that may be calculated as $\kappa_{\text{cum}}(l) = \sum_{kj} \kappa_{kj}\theta(l - l_{kj})$, where $\theta(l - l_{kj})$ — in the Heaviside function, l_{kj} is the mean free path of phonons with wave vector $\boldsymbol{k}$ and mode number j, while l is the considered upper boundary of mean free path of phonons.

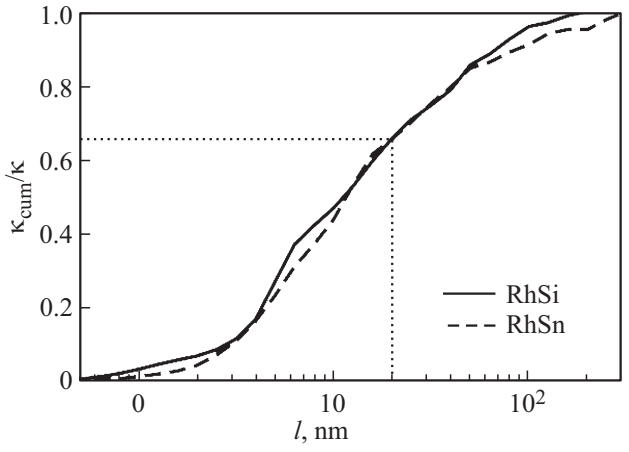

Figure 5. Dependence of cumulative thermal conductivity κ_{cum} on mean free path of phonons.

Figure 5 shows $\kappa_{\text{cum}}(l)/\kappa$. It allows to estimate the relative contribution to the lattice thermal conductivity from phonons with mean free path shorter than the given value of l. On the assumption that the contribution of phonons with larger mean free paths into heat transfer is strongly reduced due to scattering at the grain boundaries, this method makes it possible to estimate thermal conductivity reduction in nanostructured polycrystalline materials. The estimations have shown that when using this method in the given materials with grain size about 20 nm, additional reduction of lattice thermal conductivity by approximately 30% compared with the initial crystal may be expected.

Thermal conductivity for CoSi-RhSi and RhSn-RhSi substitutional solid solutions was calculated by the VC-ALD method using the obtained force constants. Thermal conductivity of solid solutions were estimated using required parameters of RhSi and RhSn calculated using PBEsol density functional. Figure 6 shows dependences of thermal conductivity on composition at room temperature. It is apparent that, when Co is substituted by a heavier element, Rh, in CoSi-based solid solutions, thermal conductivity reduction up to 2.96 W/(m · K) may be achieved in $Co_{0.3}Rh_{0.7}Si$, i. e. by more than a factor of 3.6. This is due to phonon scattering on point defects occurring when solid solutions are formed. Also it can be seen that even at small amount of substitution of Co atoms by Rh in CoSi thermal conductivity decreases considerably: by 45.4% at 5 at.% and by 54.7% at 10 at.% of Rh.

In the case of RhSi-RhSn solid solutions, a composition with 50 at.% of Sn has the lowest thermal conductivity, where thermal conductivity decreases to 1.59 W/(m · K), that is approximately 3 times as low as the lattice thermal conductivity of pure RhSi. In the case of small amount of substitution of Si atoms by Sn in RhSi, thermal conductivity will be reduced by 34.4% at 5 at.% and by 47.4% at 10 at.% of Sn.

Temperature dependences of thermal conductivity for some compositions of the given solid solutions compared with pure crystals are shown in Figure 3. The figure shows

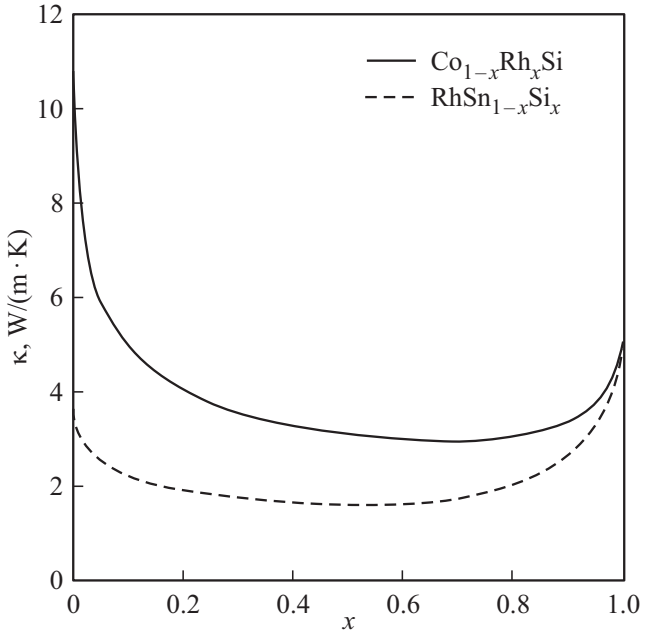

Figure 6. Dependence of lattice thermal conductivity of $Co_{1-x}Rh_xSi$ and $RhSn_{1-x}Si_x$ solid solutions on composition at $T = 300$ K.

that, for example, addition of 10 at.% of Rh to CoSi provides thermal conductivity almost like in pure RhSi in the whole considered temperature range.

It is interesting to compare the calculated values with the available experimental data. Boron-doped $Co_{1-x}Rh_xSi$ solid solutions with Rh content up to 20 at.% were studied in [27]. This study reports the lattice thermal conductivity of pure CoSi at a room temperature equal to 12.7 W/(m · K). According to other data, the lattice thermal conductivity of CoSi at room temperature vary from 10.7 to 12.7 W/(m · K) (see the references in [10]). The value of 10.8 W/(m · K) achieved herein matches the experimental data. It is 15% lower than the experimental data from [27]. The difference from the mean experimental value is about 10%. Unfortunately, the existing literature does not report any data on thermal conductivity of RhSi.

When Co was substituted by 20 at.% Rh in [27], lattice thermal conductivity appeared to be by 50% lower than that of CoSi, i. e. thermal conductivity reduction was approximately 52%. Our calculations predict a similar, but a little higher reduction of thermal conductivity with the same composition — approximately by 63%. The absolute thermal conductivities at 300 K were equal to 4 W/(m · K) which is 30% lower than the experimental value of 6 W/(m · K) [27]. Besides a possible experimental error, this deviation may be due to inaccuracy of determination of thermal conductivities in pure materials as well as due to the virtual crystal approximation and description of phonon scattering on point defects in solid solution within the framework of the perturbation theory. More accurate consideration of thermal conductivity in a solid solution may be provided using a coherent potential approximation or molecular dynamics methods and is to be considered in future.

4. Conclusion

This study performed ab initio calculation of phonon spectra and lattice thermal conductivities of RhSn and RhSi as well as thermal conductivities of CoSi-RhSi and RhSi-RhSn solid solutions. Thermal conductivity reduction is one of the ways to increase thermoelectric generator efficiency. In RhSi and RhSn, thermal conductivity at room temperature is equal to 4.9 and 3.6 W/(m · K), respectively, and appears to be much lower than that in CoSi (10.4 W/(m · K) [1]). In the given solid solutions, this value may be reduced by 3.6 times. Thus, the findings suggest that CoSi-based solid solutions with Co substituted by Rh and Si substituted by Sn may be promising for thermoelectric generator applications in terms of thermal properties of lattice.

Funding

The results were obtained using the computational resources of the supercomputer center of Peter the Great St. Petersburg Polytechnic University (www.spbstu.ru) and high-performance computer cluster of Ioffe Institute.

Conflict of interest

The authors declare that they have no conflict of interest.

References

[1] M.I. Fedorov, V.K. Zaitsev. CRC Handbook of Thermoelectrics / Ed. D.M. Rowe. Ch. 27. Boca Raton, CRC Press (1995).
[2] D.A. Pshenay-Severin, A.T. Burkov. Mater. **12**, *17*, 2710 (2019).
[3] C.S. Lue, Y.-K. Kuo, C.L. Huang, W.J. Lai. Phys. Rev. B **69**, *12*, 125111 (2004).
[4] S. Asanabe, D. Shinoda, Y. Sasaki. Phys. Rev. A **134**, *3A*, A774 (1964).
[5] A. Sakai, F. Ishii, Y. Onose, Y. Tomioka, S. Yotsuhashi, H. Adachi, N. Nagaosa, Y. Tokura. J. Phys. Soc. Jpn. **76**, *9*, 093601 (2007).
[6] H. Takizawa, T. Sato, T. Endo, M. Shimada. J. Solid State Chem. **73**, *1*, 40 (1988).
[7] N. Kanazawa, Y. Onose, Y. Shiomi, S. Ishiwata, Y. Tokura. Appl. Phys. Lett. **100**, *9*, 093902 (2012).
[8] K. Kuo, K.M. Sivakumar, S.J. Huang, C.S. Lue. J. Appl. Phys. **98**, *12*, 123510 (2005).
[9] E. Skoug, C. Zhou, Y. Pei, D.T. Morelli. Appl. Phys. Lett. **4**, *2*, 022115 (2009).
[10] D.A. Pshenay-Severin, P.P. Konstantinov, A.T. Burkov. Phys. Solid State **64**, *11*, 1685 (2022).
[11] A. Jain, S.P. Ong, G. Hautier, W. Chen, W.D. Richards, S. Dacek, S. Cholia, D. Gunter, D. Skinner, G. Ceder, K.A. Persson. APL Mater. **1**, *1*, 011002 (2013).

[12] P. Giannozzi, S. Baroni, N. Bonini, M. Calandra, R. Car, C. Cavazzoni, D. Ceresoli, G.L. Chiarotti, M. Cococcioni, I. Dabo. J. Phys.: Condens. Matter **21**, *39*, 395502 (2009).
[13] P. Giannozzi, O. Andreussi, T. Brumme, O. Bunau, M.B. Nardelli, M. Calandra, R. Car, C. Cavazzoni, D. Ceresoli, M. Cococcioni, N. Colonna, I. Carnimeo, A. Dal Corso, S. de Gironcoli, P. Delugas, R.A. DiStasio Jr, A. Ferretti, A. Floris, G. Fratesi, G. Fugallo, R. Gebauer, U. Gerstmann, F. Giustino, T. Gorni, J. Jia, M. Kawamura, H.-Y. Ko, A. Kokalj, E. Küçükbenli, M. Lazzeri, M. Marsili, N. Marzari, F. Mauri, N.L. Nguyen, H.-V. Nguyen, A. Otero-de-la-Roza, L. Paulatto, S. Poncé, D. Rocca, R. Sabatini, B. Santra, M. Schlipf, A.P. Seitsonen, A. Smogunov, I. Timrov, T. Thonhauser, P. Umari, N. Vast, X. Wu, S. Baroni. J. Phys.: Condens. Matter **29**, *46*, 465901 (2017).
[14] G. Kresse, J. Furthmuller. Phys. Rev. B **54**, *16*, 11169 (1996).
[15] G. Kresse, D. Joubert. Phys. Rev. B **59**, *3*, 1758 (1999).
[16] J.P. Perdew, K. Burke, M. Ernzerhof. Phys. Rev. Lett. **77**, *18*, 3865 (1996).
[17] J.P. Perdew, A. Ruzsinszky, G.I. Csonka, O.A. Vydrov, G.E. Scuseria, L.A. Constantin, X. Zhou, K. Burke. Phys. Rev. Lett. **100**, *13*, 136406 (2008).
[18] S. Geller, E.A. Wood. Acta Crystallogr. **7**, *Part 5*, 441 (1954).
[19] K. Schubert. Z. Naturforschung 2A, 120 (1947).
[20] A. Togo, L. Chaput, I. Tanaka. Phys. Rev. B **91**, *9*, 094306 (2015).
[21] A. Togo. J. Phys. Soc. Jpn. **92**, *1*, 012001 (2023).
[22] Z. Tian, J. Garg, K. Esfarjani, T. Shiga, J. Shiomi, G. Chen. Phys. Rev. B **85**, *18*, 184303 (2012).
[23] W. Li, L. Lindsay, D.A. Broido, D.A. Stewart, N. Mingo. Phys. Rev. B **86**, *17*, 174307 (2012).
[24] J.M. Larkin, A.J. H. McGaughey. J. Appl. Phys. **114**, *2*, 023507 (2013).
[25] J. Garg, N. Bonini, B. Kozinsky, N. Marzari. Phys. Rev. Lett. **106**, *4*, 045901 (2011).
[26] A.J. Minnich, M.S. Dresselhaus, Z.F. Ren, G. Chen. Energy Environ. Sci. **2**, *5*, 466 (2009).
[27] H. Sun, D.T. Morelli. J. Electron. Mater. **41**, *6*, 1125 (2012).

Translated by E.Ilinskaya